Journal of Colloid and Interface Science **241,** 302–316 (2001)
doi:10.1006/jcis.2001.7748, available online at http://www.idealibrary.com on IDEAL®

Surface Chemistry and Surface Charge Formation for an Alumina Powder in Ethanol with the Addition of HCl and KOH

J. Van Tassel[1] and C. A. Randall

Particulate Materials Center, Materials Research Laboratory, Pennsylvania State University, University Park, Pennsylvania 16802

Received March 14, 2001; accepted June 1, 2001; published online July 30, 2001

Surface charge and surface adsorption on an alpha-alumina powder were investigated in a 99.5/0.5 wt% ethanol/water suspension. A model is proposed in which ethanol molecules are dissociatively adsorbed as ethoxide ions and protons to Lewis acid and base sites on the surface. These ions can then desorb separately from the surface. The surface, therefore, acts as a catalyst for the autoprotolysis of the solvent and creates its own ionic atmosphere which cannot be predicted directly from chemistry in the bulk of the solvent. 3.5 μmol/m^2 of HCl is reversibly adsorbed to the surface by replacement of ethoxide ions adsorbed to surface acid sites by chloride ions. 2.4 μmol/m^2 of KOH is adsorbed to the surface by replacement of surface adsorbed protons with potassium ions. More rapid desorption of negative ions from the surface leaves the particles with a net positive surface charge except when the concentration of negative ions in solution is sufficient to supress this desorption and net surface charge goes to zero. Surface charge is found to be a function only of the activity of the negative ions in solution at the surface. No significant negative surface charge was measured under any conditions here. Equilibrium constants for surface adsorption and charge density as a function of surface activity of ethoxide and chloride ions are calculated. No effect of adsorbed potassium ions on the surface potential was found. © 2001 Academic Press

Key Words: **alumina; ethanol; zeta potential; surface potential; adsorption; surface chemistry.**

INTRODUCTION

This study is part of a larger effort to understand the process of electrophoretic deposition of particles from an electrostatically stabilized suspension. Electrophoretic deposition (EPD) is a forming process for producing particulate coatings or compact particulate bodies on an electroded surface under an electrical potential.

EPD can be divided into three basic steps. The first step is to stably suspend the particles to be deposited in a solvent. In most systems for EPD electrostatic stabilization is used. An electrostatic charge on the particle surface attracts a diffuse layer of counter ions in solution to the surface. The attraction between the charge on the surface and the counter ions in solution creates an elevated hydrostatic pressure layer around the particles. When two particles approach each other, their pressure layers provide a retarding force to keep the particles from coming within range of the strong, but short range, London–Van der Waals force which would cause the particles to stick together and sediment out of the suspension. In the second step a dc electric field is applied across the suspension causing the charged particles to migrate toward the oppositely charged electrode. With continuous application of the dc electric field the particles will accumulate at this electrode. In the final step a combination of electrostatic, electrochemical, and electrohydrodynamic effects will overcome the interparticle repulsion, the particles will come into contact, and a rigid deposition is formed.

Of the three steps in electrophoretic deposition—stabilization, electrophoresis, and deposition—the first two have been extensively studied and are well understood. The final step, deposition, where the interparticle repulsion is overcome at the electrode surface has been the subject of far fewer theoretical studies and is still not well understood. This is due in large part to the complex, dynamic, and nonequilibrium electrochemical environment near the deposition electrode. References (1–3) are some of the most notable studies that have looked at this process.

The objective of this paper is to develop a model of the surface chemical reactions on the depositing powder that will allow prediction of its behavior in the unique chemical environment near the deposition electrode. This requires knowledge of the particle adsorption isotherms for individual ions independent of the activity of their co-ions.

The alumina–ethanol system analyzed here was chosen for simplicity, stability, and the level of information available in the literature on the system components. Alumina was chosen as the powder component for its low solubility and because our own experiments showed that it could be washed easily to remove surface contaminants. Ethanol was chosen as a readily available, nontoxic solvent. Because ethanol is very hydrophilic, making and maintaining completely anhydrous ethanol is quite difficult. Therefore, ethanol with a known water content was used. Hydrochloric acid is a simple acid that is almost fully dissociated in low concentrations in ethanol, has been shown to raise the surface potential of alumina in ethanol, and has been used previously for EPD (4).

[1] To whom correspondence should be addressed. Fax: (814) 865-2326; E-mail: vantassel@psu.edu.

0021-9797/01 $35.00

Copyright © 2001 by Academic Press
All rights of reproduction in any form reserved.

MATERIALS

Alumina. The powder used in this study is AKP-50, from Sumitomo Chemical Co., Osaka, Japan. For particle size measurement the powder was dispersed in water using an ultrasonic horn, and size was measured by laser light scattering (Mastersizer, Malvern Instruments Ltd., Worcestershire, UK). The particle size distribution was bimodal with 90 vol% having an average size of 0.27 μm and 10% having an average of 3 μm. Ten vol% of the powder was less than 130 nm. Surface area as measured by single point BET (Monosorb, Quantachrome Corp., Boynton Beach, Florida) is 10.0 m^2/g. The powder is 100% α-phase by X-ray diffraction. The particles have on average symmetric with a rough, random, angular shape.

Ethanol. The ethanol used in this study is from Pharmco, Inc., Brookfield, Connecticut. The as-received water content is 0.045 wt% as determined by Fisher titration. The conductivity of the ethanol prior to water addition is less than 0.1 μS/cm. Deionized water, conductivity $\approx$0.5 μS/cm, was added to adjust the water content to 0.5 wt%. The density of this mixture is 786.6 by linear interpolation of literature data at 100% and 95% ethanol. This gives a 0.218 molar water concentration. The conductivity measured at the beginning of each of the titrations was less than 0.1 μS/cm.

HCl. Hydrochloric acid was titrated from 0.103 and 0.0103 wt% solutions in ethanol prepared by dilution of a 37 wt% HCl/water azeotropic solution (Fisher Chemical Co., Pittsburgh, Pennsylvania) into ethanol. The HCl content was verified by pH titration in water against the KOH standard solution below. Water contents as calculated from component compositions were 0.11 and 0.05 wt% for the 0.1 and 0.01 wt% solutions respectively.

KOH. A 0.098 molar potassium hydroxide standard solution in ethanol (J. T. Baker Co., Phillipsburg, NJ.) was used for titration both in as-received form and diluted by a factor of 10 using as-received ethanol above. The density of the 0.098 molar solution at 25.0°C was measured as 788.7 g/L. Water content was 0.45 wt% as determined by Karl Fisher titration. This equals a 0.197 molar water concentration.

EXPERIMENTAL METHODS

Washing and Hydration of Powder Surface

To prevent the introduction of unknown ionizable compounds into the system, the alumina powder was washed thoroughly prior to use. The powder (150 g) was placed into a 0.5 liter HDPE bottle and filled with de-ionized (D.I.) water. The bottle was heated to $\approx$60°C in a commercial microwave and shaken for $\approx$1 min. The powder was allowed to sediment out for varying lengths of time, usually overnight. The conductivity of the supernatant was measured, the supernatant was poured off, and the bottle was refilled with D.I. water. This procedure was repeated until the room temperature conductivity of the supernatant was equal to or less than the conductivity of the D.I. wash water ($\approx$0.5 μS/cm). For the powder used in this study this required nine rinsing cycles.

To verify that the powder lost when pouring off the supernatants did not affect the specific surface area, the surface area was remeasured after washing and was found to be unchanged at 10.0 m^2/g.

Thermal gravimetric analysis (TGA) of the powder after exposure to liquid water showed a discrete weight loss as it was heated from 220° to 260°C. The magnitude of this weight loss increased with time held in room temperature water and did not reach a saturation value over three days. However, by holding the powder in water at 80°C, it was found that the weight loss reached a saturation value of 0.23% in two days.

It has been reported previously that the point of zero charge of α-alumina powders in room temperature water can drift over several days from a pH of 6.7 to 9.2 (5). Water has been shown to actually reverse the charge on very well dried α-alumina in longer chain alcohols (6). To standardize the alumina surface all powder was equilibrated in 80°C water for two days after washing.

Conductivity Measurements

Conductivity was measured using a rectangular parallel plate conductivity cell having a cell constant of 0.22. The plates were of polished platinum 2.6 mm apart. The voltage across the conductivity cell was measured using a voltage divider circuit. A sine wave input signal of $\approx$1 V rms was provided by an HP 33120A signal generator. The voltage across the conductivity cell was reduced to $\approx$0.5 V rms using a resistance decade box. The total input voltage and voltage across the decade box were measured using an HP 54645A oscilloscope and used to calculate the resistance across the conductivity cell. Frequency was adjusted as a function of conductivity from 20 Hz to 20 kHz to remain between double layer capacitance effects in the conductivity cell and capacitance effects in the measuring circuit.

Calibration of the test cell and determination of absolute accuracy of the measurement procedure was performed by comparison of measurements to previously published data. Calibration was performed by titration of KCl into water using as a standard the equation of Lind *et al*. (7). This was verified and the measurement accuracy was estimated by titration of LiCl into ethanol compared to the data of Graham *et al*. (8) and Kay (9) and HCl into ethanol containing 0.5 wt% water compared to the data of De Lisi *et al*. (10). Measurement accuracy was within $\pm$1% over the range from 4 μS/cm to 120 μS/cm and within $\pm$2% from 1 to 4 μS/cm. Percentage accuracy declined rapidly below 1 μS/cm; however, absolute accuracy above 0.3 μS/cm is estimated to be within $\pm$0.05 μS/cm.

The conductivity test cell was held in the suspension with the plates aligned vertically. The bottom edge of the cell, 5.9 mm wide, was open so that powder sedimenting out of the suspension would not accumulate in the test cell. The surface conductivity of the powder can be significantly higher than that of the

bulk solution. If sedimented powder is allowed to accumulate between the plates, the higher conductivity of the sediment will short circuit the cell. A small hole in the top of one side of the cell allowed for free circulation of suspension through the cell.

Titration Procedure

Conductumetric and pH titrations were performed in a jacketed beaker maintained at $25 \pm 0.02^{\circ}$C by a circulating isothermal bath. Titrants were added manually by weight. Where alumina was added, it was first held in a drying oven at 135°C for at least 2 h to standardize the quantity of adsorbed water. In all cases alumina was added to yield an approximately 1 vol% suspension.

The solution was mixed using a magnetic stirrer. The powder was sufficiently flocced from the washing process that it rapidly sedimented out at all conditions when the stirrer was turned off. Conductivity measurements made with the powder held in suspension by stirring and in the quiescent supernatant after sedimentation were identical within the measurement error of the apparatus and technique.

Electrophoretic Mobility

Mobility was measured using a Delsa 440 laser doppler velocimeter (Beckman Coulter, Inc., Fullerton, California). This instrument measures particle velocity in suspension within a rectangular capillary. An electric field of 57 V/cm is applied across the capillary for 2.5 s turned off for 2 s, applied again in the reverse direction for 2.5 s. This is repeated 12 times and the results are averaged. Reversing the field is intended to minimize the electrochemical double layer formation at the electrodes. If the velocity measured in each polarization direction was not the same, the measurement was rejected.

To separate the electro-osmotic flow of the fluid in the capillary from the electrophoretic motion of the particles, particle velocity was measured at nine points across the capillary, the results were fitted to a parabola, and the particle velocities at the theoretical stationary levels were calculated from the parabola. For all of the data points reported here the r^2 fit of the parabola was better than 98%.

For a significant signal to be generated by the instrument the laser must be able to propagate across the capillary with only modest scattering. This requires that the sample have a volume density of particles in suspension of 0.01% vs 1% in the standard working suspensions used here. To prepare samples for measurement a 1% suspension was prepared in a centrifuge tube. HCl solution was added, the suspension was mixed, and conductivity was measured to determine the ionic strength in the solvent. The suspension was centrifuged at 3600 m/s^2 for 3 min. This usually left enough particles suspended in the supernatant for an electrophoretic measurement. If there were too few particles in the supernatant, some of the clear supernatant was drawn into a syringe, the remaining material was resuspended, and a small amount was drawn into the same syringe and mixed. Volume density was judged visually.

We were only able to produce credible measurements using this instrument for very stable suspensions that were also stabilized against flocculating to the quartz capillary wall. Although there was no attempt to quantify the surface charge on the capillary walls, in all of the measurements where a stable, symmetric, parabolic electro-osmotic flow developed the flow indicated that there was a significant positive charge on both the capillary walls and the particles. Without this stability, the horizontal capillary is susceptible to sedimentation of particles onto the bottom surface. This gives the bottom a different surface charge from the top and prevents the development of a symmetric parabolic flow. As a result we were unable to make any valid measurements in suspensions with added KOH.

Electroacoustic Measurement

These measurements were made using an ElectroAcoustic Spectrometer DT-1200 with automatic titrator (Dispersion Technology, Inc., Mt. Kisco, New York). This instrument uses a piezoelectric actuator to apply a 1 MHz acoustic signal to a particulate suspension. Because of the density difference between the particles and solvent, there will be a relative motion between the two in the acoustic wave. This relative motion polarizes the electrostatic double layer around the particles. This polarization is detected as a current at an electrode on the face of the acoustic actuator.

To prepare the suspensions for electroacoustic measurement the alumina powder was placed in a 135°C oven for 2 h to standardize the adsorbed water. This was added to the 99.5/0.5 wt% ethanol/water solvent to produce a 1.00 vol% alumina suspension. The mixture was placed on a vibratory mill for ≈6 h with 2 mm spherical alumina milling media. The HCl titration was performed the next day and the KOH titration was performed on a portion of the same suspension one day later. The suspension was very stable and the initial zeta potential reading for each titration was within ±1 mV.

The instrument was calibrated with a 10 vol% silica Ludox suspension with a zeta potential of −38 mV in water measured independently with an optical zeta potential instrument. Readings were made in a partially covered beaker rapidly and continuously stirred with a magnetic stir bar at ambient temperature, $25^{\circ} \pm 3^{\circ}$C. An automatic titrator was used to inject fixed volumes of titrant. In the titration with HCl, the suspension was allowed to equilibrate for 5 min after each injection of HCl solution before two zeta potential readings were made, each 40 s apart. In the KOH titration the equilibration time was reduced to 2 min.

pH

The pH numbers reported here are the direct numerical reading measured using a Fisher Accumet 20 pH meter (Fisher Scientific, Pittsburgh, Pennsylvania). An Accumet combination probe was used consisting of a general purpose glass sensing membrane and a Ag/AgCl reference electrode with a porous plug junction. The meter was calibrated using aqueous standard

buffers at pH 4.00, 7.00, and 10.00. Below a conductivity of ≈1 μS/cm pH readings were not stable. Above this conductivity and below readings of ≈pH 9 stable reproducible readings were produced within 3 min of imersion in the ethanol. When the probe was replaced in the aqueous standard it returned within 1 min to the standard value. Above readings of ≈pH 9 there was considerable drift in the readings and when the probe was returned to an aqueous standard up to 20 min could elapse before the probe returned to the correct reading.

RESULTS AND DISCUSSION

Surface Charge and Adsorption with the Addition of HCl

Zeta potential. Mobilities measured by electrophoresis are given in Table 1. Without an independent mobility standard in ethanol the accuracy of the measurements could not be estimated; however, when a symmetric electro-osmotic flow profile was established in the measurement capillary, reproducibility was within ±5%.

The conductivity was measured using a commercial parallel plate conductivity cell with a cell constant of 0.107 cm^{-1}. The edges of the cell were open and, therefore, due to edge effects there is a great deal of uncertainty in the conductivity measurements below 4 μS/cm. Above this the estimated accuracy is ±10%. The first point represents only the washed alumina in ethanol with no added HCl and no conductivity measurement was made. Previous measurements of this concentration of alumina in ethanol have shown conductivity less than 0.05 μS/cm.

The molar ionic concentration in the bulk solution was then calculated with the Fuoss–Onsager equation (11) using values for HCl in 99.5 wt% ethanol linearly interpolated from the data of De Lisi *et al.* (10) taken at 99.60 and 99.41 wt% ethanol: $\Lambda_O = 53.40$, $a_O = 3.64$, and $K_A = 21$.

The bulk molar ionic strength was then used to calculate the Debye length,

$$\kappa = \left[\frac{2e^2\rho_\infty z^2}{\varepsilon_o\,\varepsilon_r\,kT}\right]^{\frac{1}{2}}. \qquad [1]$$

The relative double layer thickness, κa, was calculated using the average particle radius of 150 nm. The nondimensional reduced mobility, **E**, was calculated from the electrophoretic mobility, u_E,

$$\mathbf{E} = \frac{3\eta e}{2\varepsilon_r\varepsilon_o KT}\cdot u_E. \qquad [2]$$

These values were then used to find the reduced potential, $\tilde{\zeta}$, graphically from the charts for a 1:1 electrolyte published by O'Brien and White (12). The zeta potential was then calculated in mv using

$$\tilde{\zeta} = \frac{ez\zeta}{kT}. \qquad [3]$$

(Definitions of the terms used in these and all subsequent equations can be found in the appendix.)

Zeta potential was also measured using an electroacoustic instrument that measures the colloid vibration current and calculates the particle zeta potential based on a thin double layer assumption. The inputs to this instrument are the suspension volume fraction, solvent and particle densities, and average particle size. The instrument controls an automatic titrator and its output is the volume of an HCl solution titrated into the suspension and the calculated zeta potential.

The quantity of acid titrated into the suspension was first converted into bulk concentration of HCl by interpolation of the raw adsorption data as shown in the section on acid adsorption below. Using the resulting zeta potential vs bulk ionic strength a chloride adsorption isotherm was calculated and used to recalculate the bulk ionic strength from the quantity of acid titrated in. These data were then used as the bulk free molarity of HCl on the horizontal axis in Fig. 1.

Concurrent with the calculation of bulk ionic strength, the zeta potential must be adjusted for double layer thickness effects. The zeta potential reported by the instrument is calculated based on a thin boundary layer assumption (13) and significantly underestimates the actual zeta potential for the range of double layer thicknesses considered here ($\kappa a \approx 1$–20). Sawatzky and Babchin (14) have developed a theory for arbitrary double layer thickness. A key component of this theory is a function, not reproduced here, $f_1(\kappa a, a/\delta)$, which gives the ratio of the actual dynamic electrophoretic mobility to the mobility calculated

TABLE 1
Properties of α-Alumina Powder Suspensions

Conductivity (μS/cm)	Bulk molarity (mM)	Debye length (nm)	κa	Mobility (μm · cm/V · s)	Reduced mobility	Reduced potential	Potential (mV)
<0.1			<1	0.81	2.27	2.36	61
0.46	0.009	58.5	2.6	1.00	2.80	3.55	91
1.23	0.023	36.0	4.2	1.00	2.80	3.38	87
4.91	0.095	17.7	8.5	0.88	2.46	2.28	59
12.02	0.242	11.1	13.5	0.84	2.35	1.97	51
19.81	0.400	8.6	17.4	0.74	2.07	1.65	42

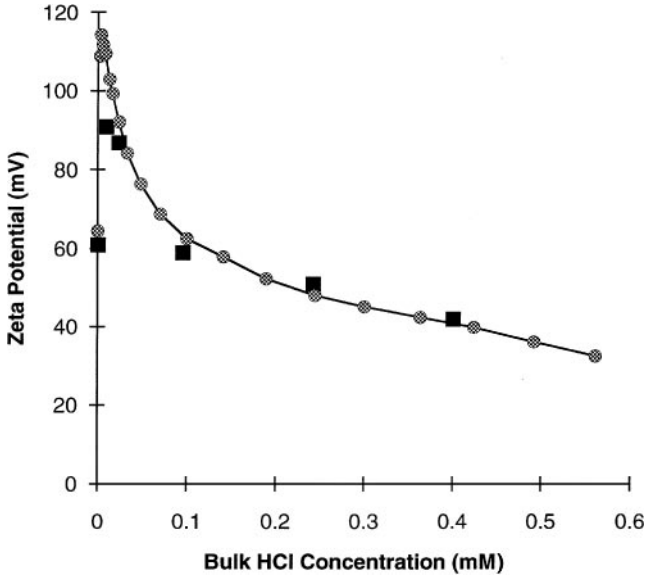

FIG. 1. Zeta potential vs bulk HCl concentration. Solid squares are zeta potentials calculated from electrophoretic mobility; circles are calculated from electroacoustic current using thin boundary layer theory and adjusted using the correction factor of Henry (15).

assuming a thin double layer. The parameter

$$\delta = \left(\frac{2\eta}{\rho\omega}\right)^{\frac{1}{2}} \qquad [4]$$

is a characteristic distance related to the distance over which the pressure waves generated by an oscillating particle decay. As the parameter $a/\delta \to 0$ the function f_1 goes to the function $f(\kappa a)$ of Henry (15) for calculating the dc electrophoretic mobility of particles with intermediate thickness double layers. The electroacoustic measurements used here were performed at a frequency of 1 MHz, which for ethanol will give a value for δ of 1.65 μm. Using the average particle radius, a, of 0.15 μm and evaluating f_1 at its limits shows that the error in using the adjustment factor of Henry over the more complex formulation of Sawatzky and Babchin is everywhere less than 10%. Therefore the adjustment of zeta potential values was done using values for the Henry formula interpolated from tabulated values. The resulting values, shown in Fig. 1, show the agreement between the different zeta potential measurement methods.

When these data are replotted as a function of $-\log_{10}$ of the concentration of HCl in the bulk solution it appears reasonable that for bulk molar concentrations of HCl greater than 10 μM the zeta potential can be modeled as a straight line. Since the deviation between the straight line model and the data is less than the expected error in measuring and calculating the zeta potential ($\approx$10%), values from the straight line approximation will be used in the subsequent calculations.

Surface charge. Given the surface potential and the bulk ionic strength of the solvent, the surface charge density can be calculated. Loeb *et al*. (16) used a numerical algorithm to calculate the surface charge density of a spherical colloid particle for a range of potentials and double layer thicknesses. They also presented an empirical formula,

$$q = \frac{\varepsilon_0\,\varepsilon_r\,kT}{e}\kappa\left(2\sinh\left(\frac{1}{2}\tilde{\zeta}\right) + \frac{4}{\kappa a}\tanh\left(\frac{1}{4}\tilde{\zeta}\right)\right), \qquad [5]$$

that can be used to estimate the results of their numerical calculations for surface charge density in a 1–1 electrolyte system to within 1% for the range of potential and double layer thickness values being considered here. We have used this equation to calculate the particle surface charge density, q, in mC/m^2 for the zeta potentials shown in Fig. 2. The results are shown on the graph in Fig. 3. These values were calculated using the linear zeta potential approximation except for the three data points below 10 μM HCl, which diverge from the linear model. These points were calculated directly from the adjusted electroacoustic data and are shown as circles on the graph in Fig. 3.

Acid adsorption. Adsorption of HCl to the powder surface was determined using conductivity measurements. HCl was titrated into the 99.5/0.5 wt% ethanol/water solvent mixture without alumina. This conductivity as a function of HCl addition is shown as round points in Fig. 4. The line labeled (1) superimposed on these points is the predicted conductivity/concentration curve using the Fuoss–Onsager equation (11) for an associated electrolyte,

$$\Lambda = \Lambda_0 - S(c\alpha)^{1/2} + E'c\alpha\ln(6E_1'c\alpha) + Lc\alpha - K_A c\alpha\,\gamma_{\pm}^2\Lambda. \qquad [6]$$

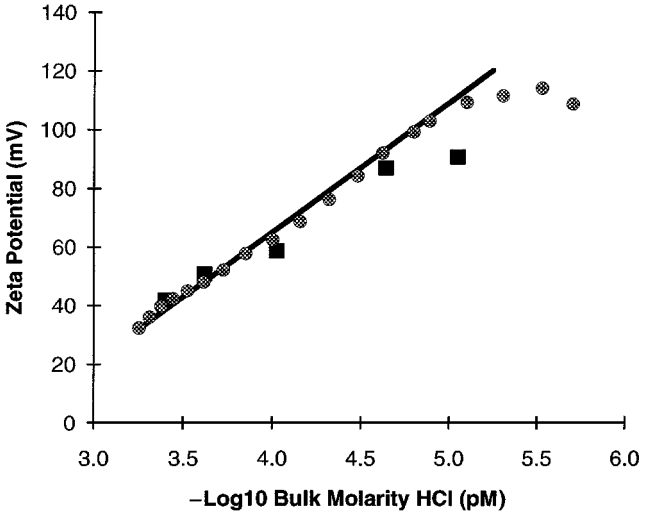

FIG. 2. Zeta potential vs bulk molarity of HCl. Solid squares are zeta potentials calculated from electrophoretic mobility; circles are calculated from electroacoustic current using thin boundary layer theory and adjusted using the correction factor of Henry (15).

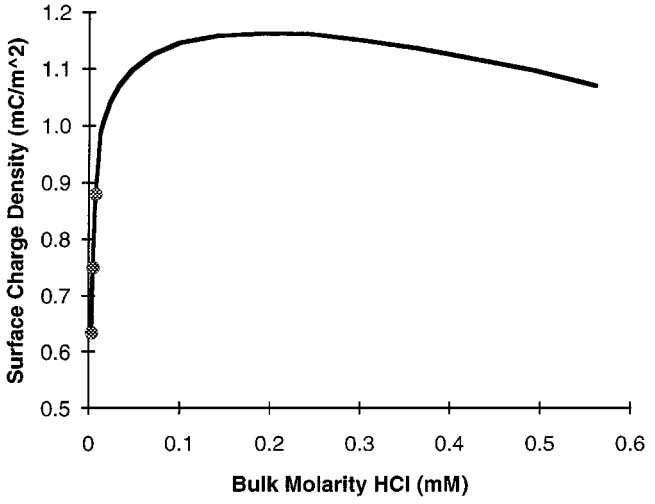

FIG. 3. Surface charge density millicoulombs/m^2. Circles are data points for bulk molarity less than 10 μM that do not correspond to the linear approximation shown in Fig. 2.

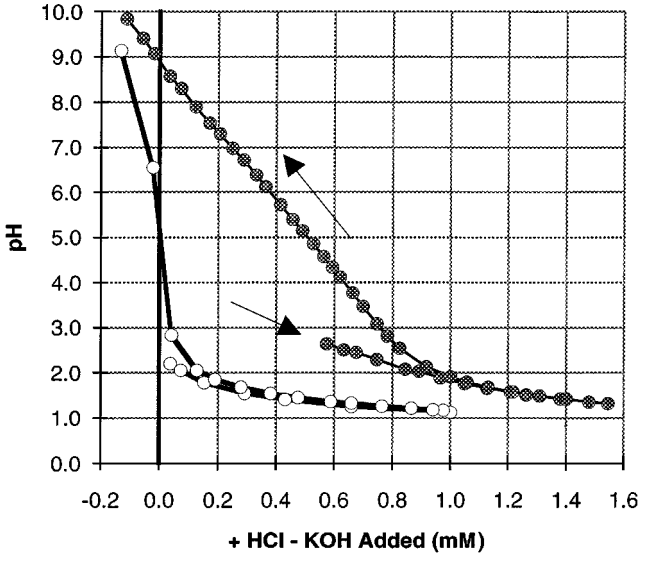

FIG. 5. Indicated pH in ethanol +0.5 wt% water, forward titration with HCl, and back titration with KOH. Open circles are for ethanol only, filled circles are for ethanol plus 1 vol% alumina powder; surface area ≈2 m^2/liter.

It is calculated using values for HCl in 99.5 wt% ethanol linearly interpolated from the data of De Lisi *et al.* (10) as reported above.

The square data points in Fig. 4 are for the same conditions with the addition of 1 vol% alumina powder. The molarity of HCl in the solution is calculated from the conductivity. The difference between the HCl in solution and the total HCl titrated is taken to be the surface adsorption of the powder.

Reversibility of adsorption. Although the disappearance of HCl from solution in the presence of alumina can be measured accurately by conductumetry, the question remains whether this is by surface adsorption or by an irreversible chemical reaction either changing the composition of the surface or converting the HCl to nonionizing species in solution.

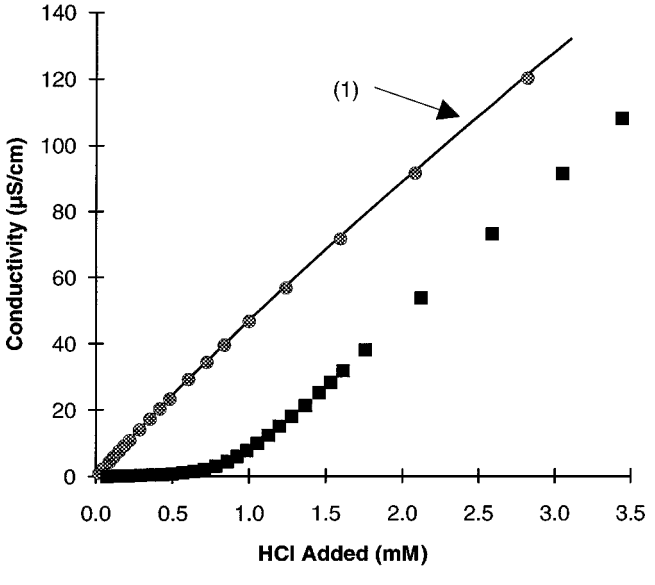

FIG. 4. Solution conductivity with and without alumina powder present. Line labeled (1) is Fuoss–Onsager equation [6] plotted based on data from De Lisi *et al.* (10).

The reversibility of the adsorption was tested by pH titration as shown in Fig. 5. HCl was titrated into ethanol with and without alumina. pH readings were unstable until a concentration of HCl in solution of 0.02 mM was reached (conductivity ≈1 μS/cm). Above that the difference between the HCl titrated with and without alumina at equal pH readings confirms the adsorption of HCl as determined by conductivity. Back titration of the solutions with KOH then shows the buffering of the pH change in the alumina suspension due to the adsorbed HCl.

As a further check for other chemical reactions, the supernatants of alumina suspensions were checked by plasma spectroscopy for dissolved species containing aluminum. Suspensions of alumina in ethanol were prepared in ethanol alone, ethanol with up to 0.5 mM KOH, and ethanol with up to 2.5 mM added HCl. Supernatant was removed from the samples 2 h, 1 day, and 10 days after preparation for analysis. No aluminum was detected in the solvent from any of the samples above a 90% confidence level minimum detection limit of 0.05 mM aluminum. This indicates that the adsorption does not involve reactions leading to a significant dissolution of aluminum from the surface.

Notes on concepts and terminology. Before beginning further analysis of the data it will be useful to define some of the basic concepts used here regarding the surface, diffuse layer, and solution chemistry in an ethanol–water solvent.

The particle is presumed to have a fixed number of surface sites, which are unoccupied, occupied by a proton, or occupied

by a proton and a negative ion. There are neither assumptions about the nature of the bonding nor invocation of an electrostatically bonded Stern or Helmholtz layer. All ions that are not adsorbed to a surface site are presumed to be in solution and outside the shear plane. Thus the terms "on the surface" or "adsorbed to the surface" imply ions that are rigidly attached to the particle surface and are inside the shear plane for electrophoretic measurement. The term "at the surface" is then used to imply activities and potentials immediately adjacent to the surface but for ions still dissolved and moving freely in the solvent, and therefore outside the shear plane. As a result, the zeta potential, the potential measured at the shear surface, will be assumed to be equal to the surface potential.

The standard continuum assumptions are made: first that the surface charge is continuous across the surface and second that the solvent is a continuous dielectric medium with the ions behaving as point charges. The second assumption seems reasonable given that at the maximum ionic strength where we have measured a zeta potential the Debye length is 7.3 nm, about 20 times the 3.65 Å distance of closest approach of oppositely charged ions in solution determined by conductumetry. The assumption that is likely to be violated first is that of a uniform, continuous surface charge. For the measurements with HCl the calculated surface charge of $\approx$1 mC/m^2 translates to one positive charge per 160 nm^2 or a uniformly distributed charge–charge separation distance of 13 nm. This is close to twice the Debye length mentioned above.

Notation in square brackets indicates either volume concentration in mol/m^3 (mM) or surface concentration in mol/m^2. The activity of ions in the bulk solution is calculated as the product of the concentration and the Debye–Hückel activity correction factor, $\gamma_\pm$, calculated using

$$-\ln \gamma_\pm = \frac{\kappa e^2}{8\pi \varepsilon_o \varepsilon_r kT(1+\kappa a_o)}. \qquad [7]$$

If the particle surface is charged there will be separate activity correction factors for positive and negative ions, γ_+ and γ_-, at the surface since in this region the solution is not charge balanced. There will be no attempt to calculate either these correction factors or the surface ionic concentrations. Only the product of the two, the surface activity, will be calculated from the bulk activity using the Boltzmann relation, Eq. [11].

Finally, a note on the behavior of acids and bases in ethanol–water solvents is needed. In the case of a Brønsted acid, the proton will have a greater affinity for water molecules in the solvent. Based on the equilibrium constant calculated in (10), in a 99.5/0.5 wt% ethanol/water solvent mixture the protonated species will be 70 wt% H_3O^+ and 30 wt% H_2EtO^+. For a Brønsted base such as KOH in the same solvent mixture the negative ions will be 96 wt% ethoxide and the balance hydroxide, based on the equilibrium constant in (18). In the following discussion references to hydronium and ethoxide ions will implicitly include equilibrium concentrations of the protonated ethanol and hydroxide ions, respectively.

Modeling adsorption and surface charge with HCl. When the alumina powder is first put into the ethanol it develops a significant surface charge. The hypothesis for the development of this charge is that sites on the alumina surface act as a Lewis base, an electron donor. Ethanol molecules are adsorbed to these sites by their polar hydroxyl group:

$$\mathrm{Ss} + \mathrm{HEtO} \rightleftharpoons \mathrm{Ss}\cdot\mathrm{H}^+\cdot\mathrm{EtO}^-.$$

There is then an equilibrium dissolution of ethoxide ions from the surface, leaving protonated surface sites and a positive surface charge. The equilibrium for this reaction is given by

$$\mathrm{Ss}\cdot\mathrm{H}^+\cdot\mathrm{EtO}^- \rightleftharpoons \mathrm{Ss}\cdot\mathrm{H}^+ + \mathrm{EtO}_S^-, \qquad K_1 = \frac{[\mathrm{Ss}\cdot\mathrm{H}^+]\gamma_-[\mathrm{EtO}_S^-]}{[\mathrm{Ss}\cdot\mathrm{H}^+\cdot\mathrm{EtO}^-]}. \qquad [8]$$

As HCl is added to the suspension there is a very rapid rise in the surface charge and in the zeta potential. This is likely due to a sharp reduction of ethoxide concentration in the bulk of the solvent due to reaction with the added HCl:

$$\mathrm{EtO}_B^- + \mathrm{H}_B^+ \rightleftharpoons \mathrm{HEtO}.$$

The $-\log_{10}$ of the equilibrium constant for this reaction, pK_S, is 19 for pure ethanol (17) and 18 for a 90/10 ethanol/water mixture (18).

Simultaneously there is an adsorption of chloride ions to the surface by substitution of chloride for the ethoxide ions at the surface. Surface charge now becomes principally a function of the equilibrium dissolution of chloride ions from the surface:

$$\mathrm{Ss}\cdot\mathrm{H}^+\cdot\mathrm{Cl}^- \rightleftharpoons \mathrm{Ss}\cdot\mathrm{H}^+ + \mathrm{Cl}_S^-, \qquad K_2 = \frac{[\mathrm{Ss}\cdot\mathrm{H}^+]\gamma_-[\mathrm{Cl}_S^-]}{[\mathrm{Ss}\cdot\mathrm{H}^+\cdot\mathrm{Cl}^-]}. \qquad [9]$$

Equations [8] and [9] can be combined to yield

$$\frac{[\mathrm{Ss}\cdot\mathrm{H}^+\cdot\mathrm{Cl}^-]}{[\mathrm{Ss}\cdot\mathrm{H}^+\cdot\mathrm{EtO}^-]} = \frac{K_1}{K_2}\frac{\gamma_-[\mathrm{Cl}_S^-]}{\gamma_-[\mathrm{EtO}_S^-]}. \qquad [10]$$

This shows that the adsorption of chloride can be modeled as a substitution of a chloride ion for an ethoxide ion on the surface, with the adsorption ratio determined by the ratio of dissolved chloride to ethoxide at the surface.

From conductivity measurements we know the bulk activity of the chloride ion, and with the zeta potential, the surface activity of chloride can be calculated using the Boltzman relationship and the bulk activity coefficient,

$$\gamma_-[\mathrm{Cl}_S^-] = \gamma_\pm[\mathrm{Cl}_B^-]\exp\left(\frac{e\zeta}{kT}\right). \qquad [11]$$

Then it will be assumed *a posteriori* that the surface ethoxide concentration can be estimated as a constant multiplied by an exponential of the zeta potential:

$$\gamma_{-}[\mathrm{EtO_S^-}] = K_{\mathrm{EtO}} \exp\left(\frac{e\zeta}{2kT}\right). \quad [12]$$

Substituting [11] and [12] into [10] we generate an equilibrium equation in which the ratio of chloride to ethoxide adsorbed to the surface is a function of a constant and a lumped parameter, which is the bulk chloride concentration times an exponential of the zeta potential, as shown in the following equation:

$$\frac{[\mathrm{Ss}\cdot\mathrm{H^+}\cdot\mathrm{Cl^-}]}{[\mathrm{Ss}\cdot\mathrm{H^+}\cdot\mathrm{EtO^-}]\gamma_{\pm}[\mathrm{Cl_B^-}]\exp\left(\frac{e\zeta}{2kT}\right)} = \frac{K_1}{K_2 K_{\mathrm{EtO}}}. \quad [13]$$

To simplify the following equations we collect all of the constants into one lumped parameter and write a simplified expression for the chloride dependence:

$$K_{\mathrm{L}} = \frac{K_1}{K_2 K_{\mathrm{EtO}}} \quad [14]$$

$$f(\mathrm{Cl}) = \gamma \pm [\mathrm{Cl_B^-}] \exp\left(\frac{e\zeta}{2kT}\right) \quad [15]$$

Note that the function $f(\mathrm{Cl})$ depends on both the bulk chloride concentration and the zeta potential.

Assuming that there are a fixed number of surface sites and that these can be broken down into sites that are occupied by an ethanol molecule, HCl, a proton or are unoccupied, the total surface site concentration is given by

$$[\mathrm{Ss_{Tot}}] = [\mathrm{Ss}\cdot\mathrm{H^+}\cdot\mathrm{EtO^-}] + [\mathrm{Ss}\cdot\mathrm{H^+}\cdot\mathrm{Cl^-}] + [\mathrm{Ss}\cdot\mathrm{H^+}] + [\mathrm{Ss}]. \quad [16]$$

A further approximation can be made assuming that the number of surface sites that are only occupied by a proton or are unoccupied are small relative to the total number of surface sites. With these approximations Eqs. [14]–[16] can be substituted into Eq. [13] and algebraically manipulated to obtain an equation in the form of a Langmuir adsorption isotherm:

$$[\mathrm{Ss}\cdot\mathrm{H^+}\cdot\mathrm{Cl^-}] = \mathrm{Ss_{Tot}}\frac{K_{\mathrm{L}} f(\mathrm{Cl})}{1 + K_{\mathrm{L}} f(\mathrm{Cl})}. \quad [17]$$

By plotting the inverse of this equation,

$$[\mathrm{Ss}\cdot\mathrm{H^+}\cdot\mathrm{Cl^-}]^{-1} = \mathrm{Ss_{Tot}^{-1}} + (K_{\mathrm{L}}\mathrm{Ss_{Tot}} f(\mathrm{Cl}))^{-1}, \quad [18]$$

which is linear, the values for the total number of surface sites and the lumped equilibrium parameter K_{L} can be estimated by a least-squares fitting. This is plotted in Fig. 6a for data points taken at conductivities above 2 μS/cm ($\approx$0.04 mM bulk molar concentration). The resulting values are $\mathrm{Ss_{Tot}} = 3.48$ μmol/m^2 and $K_{\mathrm{L}} = 7.7$. The direct form of the equation, Eq. [17], is plotted using these parameters and is shown in Fig. 6b. The actual adsorption data points are superimposed on this curve showing the level of fit.

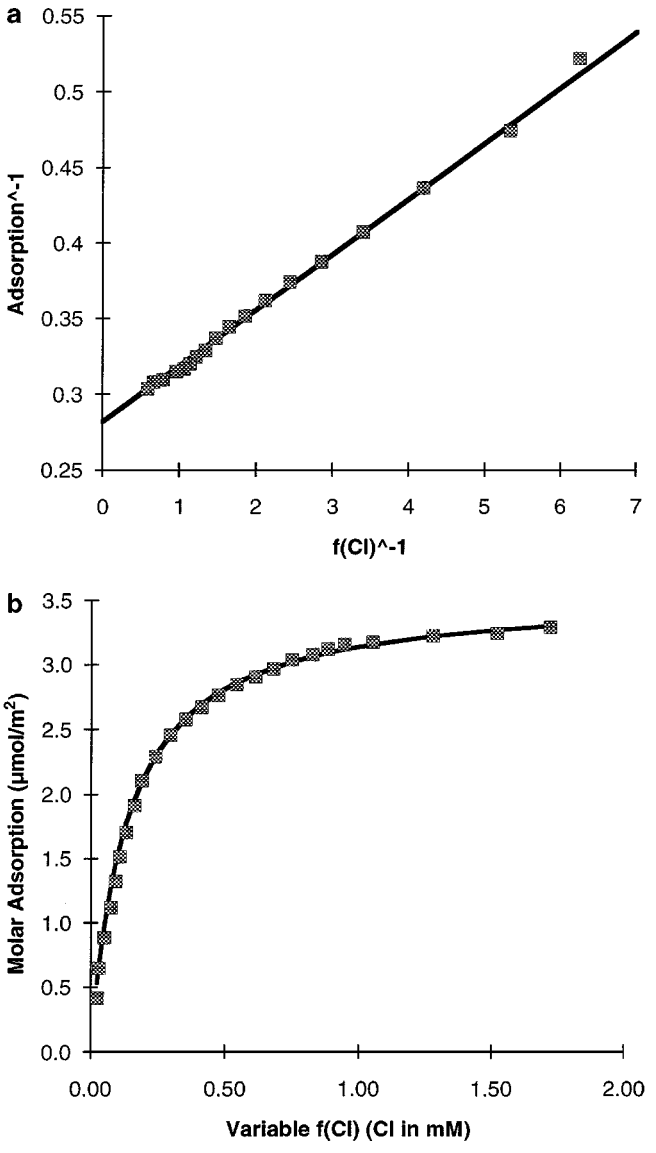

FIG. 6. (a) Inverse of surface adsorption data for bulk molar HCl concentrations above 0.04 mM plotted as a function of the inverse of Eq. [15]. The straight line is fitted by least squares. (b) Surface adsorption data plotted as a function of Eq. [15] superimposed on a fitted plot of the adsorption isotherm, Eq. [17].

Having developed an equation which accurately describes the chloride adsorption, it is now necessary to review the assumptions that were made in the derivation.

The assumption that the number of surface sites occupied only by a proton is small relative to the total number of surface sites does appear reasonable. The maximum surface charge density measured here is 1.14 mC/m^2 or 11.8 nmol/m^2. This is 0.34%

of the total number of surface sites estimated by the chloride adsorption isotherm.

The assumption that the number of unoccupied surface sites is small is more difficult to address as there is no direct measurement of empty surface sites. However, if the equilibrium constant for the dissolution of an ethanol molecule from a surface site,

$$\mathrm{Ss \cdot H^+ \cdot EtO^- \rightleftharpoons Ss + HEtO}, \qquad [19]$$

is significantly larger than the equilibrium constant for the removal of a proton from a surface site by either an ethanol or water molecule,

$$\mathrm{Ss \cdot H^+ + H_2O \rightleftharpoons Ss + H_3O^+}, \qquad [20]$$

it can be shown that the concentration of empty surface sites will not affect the results derived here.

The assumption that there are a fixed number of surface sites is supported by the excellent fit of the adsorption data to a standard isotherm model.

It was also assumed that there is an equilibrium among the surface charge, free chloride ion concentration at the surface, and the total adsorbed chloride. If this is true the value of K_2 calculated from Eq. [9] should be a constant over the range where there is a significant level of chloride adsorbed to the surface.

As can be seen from the plot in Fig. 7, the calculated value of K_2 varies by $\approx\pm 10\%$; however, although the denominator is known to within a percent over most of the range, the numerator is the product of two values that are an exponential function of the zeta potential. This makes the calculated value of this function very sensitive to the magnitude of the zeta potential. A change of 5% in the value of the zeta potential at 100 mV leads to a 30% change in the calculated value of K_2. This sensitivity to a $\pm 5\%$ change in the zeta potential is also plotted in Fig. 7.

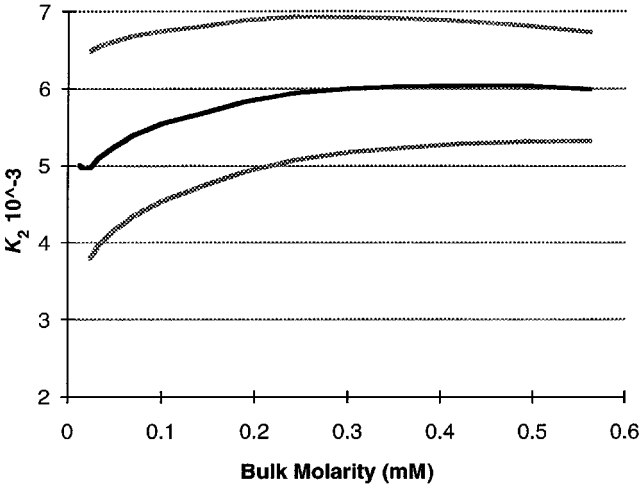

FIG. 7. Plot of K_2 from Eq. [9]. Quantities are in moles or mol/m^2, as appropriate. Gray lines show the sensitivity of the calculation to a $\pm 5\%$ change in zeta potential.

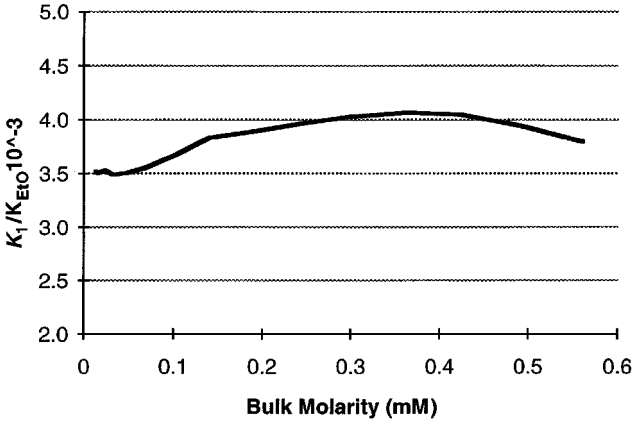

FIG. 8. Plot of K_1/K_{EtO} from Eqs. [8] and [12]. Variation around the average value is $\pm 8\%$.

While the data do not conclusively prove that K_2 is a constant, this assumption seems reasonable and is well within the limits of measurement error for the data used here.

Justification of the next two assumptions is somewhat more involved, and they will be treated together. The first is that there is an equilibrium among surface adsorbed ethanol, protonated surface sites, and dissolved ethoxide ions at the surface (eq. [8]). The second is that the concentration of the ethoxide ion at the surface changes in proportion to the square root of the Boltzmann relation of the zeta potential (Eq. [12]).

One way of testing these assumptions is to substitute Eq. [12] into Eq. [8] and calculate the value K_1/K_{EtO} to see how closely this approximates a constant over the range of HCl concentrations used here. The result of this calculation as shown in Fig. 8 is within $\pm 8\%$ of a constant. As with K_2 above, this is a very sensitive function of zeta potential and the assumption that the value K_1/K_{EtO} is a constant does not appear unreasonable.

Although a theoretical justification can be made for why the surface concentration of the ethoxide ion should be approximated by Eq. [12], the best test of this assumption is to return to Eq. [10], substitute Eq. [8] for the surface ethoxide concentration, and recalculate the adsorption isotherm. Although there are insufficient data to estimate the absolute ethoxide concentration at the surface, and therefore a value for K_1, the adsorption can be plotted as a function of the surface chloride concentration divided by the ethoxide concentration over K_1. To do this, Eq. [18] is replotted replacing $f(\mathrm{Cl})$ with $f'(\mathrm{Cl})$ given by

$$f'(\mathrm{Cl}) = \frac{\gamma_{\pm}[\mathrm{Cl_B^-}]\exp\left(\frac{e\zeta}{kT}\right)}{(\gamma_{-}[\mathrm{EtO_S^-}]/K_1)} = \frac{[\mathrm{Ss \cdot H^+}] \times \gamma_{\pm}[\mathrm{Cl_B^-}]\exp\left(\frac{e\zeta}{kT}\right)}{[\mathrm{Ss_{Tot}}] - [\mathrm{Ss \cdot H^+ \cdot Cl^-}]} \qquad [21]$$

(Fig. 9). The fit to a straight line is slightly worse than shown in Fig. 5, particularly at the extrema; however, the assumption embodied in Eq. [12] has been eliminated and it has been shown

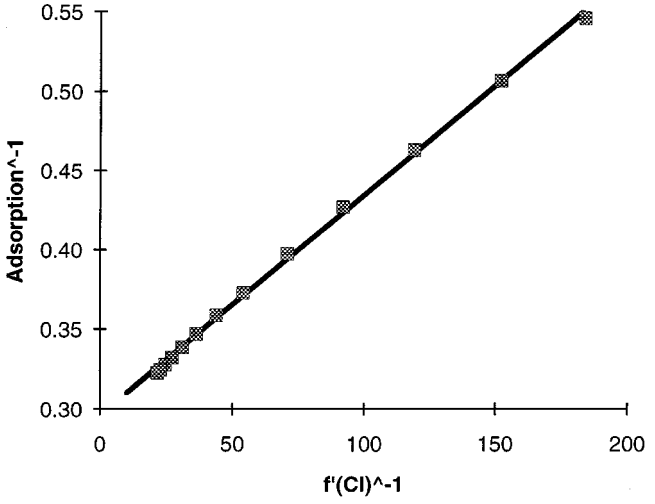

FIG. 9. Inverse of surface adsorption data for bulk molar HCl concentrations above 0.04 mM plotted as a function of the inverse of Eq. [21]. The straight line is fitted by least squares.

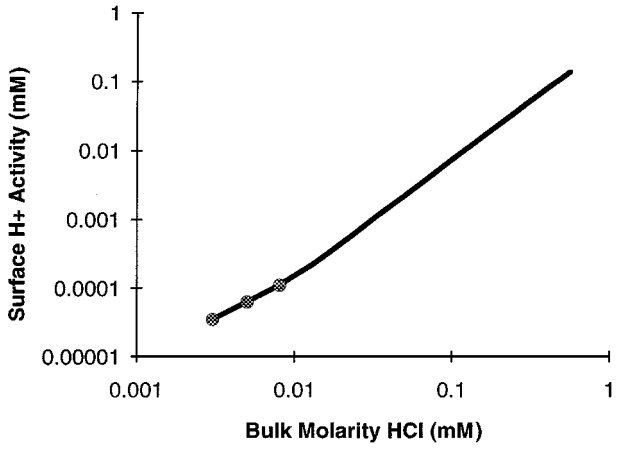

FIG. 10. Log/log plot of surface activity of H^+ ion calculated from bulk concentration using the Boltzmann relation.

that surface charge and the adsorption of HCl to the surface can be modeled using only the very basic Eqs. [8], [9], and [16].

The one significant reaction that has not yet entered into the discussion is the autoprotolysis equilibrium for ethanol,

$$\begin{aligned} \mathrm{HEtO} &\rightleftharpoons \mathrm{EtO_B^-} + \mathrm{H_B^+}, \\ K_S &= \frac{\gamma_\pm^2[\mathrm{H^+}][\mathrm{EtO^-}]}{[\mathrm{HEtO}]}. \end{aligned} \qquad [22]$$

This controls the ethoxide ion concentration given the concentration of the protonated species and vice versa. If the surface proton activity is calculated from the bulk concentration and zeta potential using the Boltzmann relation,

$$\gamma_+[\mathrm{H_S^+}] = \gamma_\pm[\mathrm{H_B^+}]\exp\left(\frac{-e\zeta}{kT}\right), \qquad [23]$$

this activity would be expected to rise by four orders of magnitude over the measurement range, as plotted in Fig. 10. If the autoprotolysis equilibrium equation (Eq. [22]) is valid at the surface, then the activity of the ethoxide ion at the surface would be expected to decline proportionally by four orders of magnitude.

That, however, contradicts the model developed above where the ethoxide concentration at the surface is set by a surface equilibrium reaction. The relative change in ethoxide concentration can be plotted from a combination of Eqs. [8] and [16] Eq. [8, 16]. This is shown in Fig. 11, where the ethoxide concentration is seen to change by only one order of magnitude. Even further, over the range of bulk HCl concentrations from 0.01 to 0.56 mM, the predicted concentration of the proton at the surface is seen in Fig. 10 to increase by a factor of more than 1000 while the relative ethoxide concentration as shown in Fig. 11 declines by less than a factor of 7.

$$\frac{\gamma_-[\mathrm{EtO_S^-}]}{\mathrm{K_1}} = \frac{[\mathrm{Ss_{Tot}}] - [\mathrm{Ss}\cdot\mathrm{H^+}\cdot\mathrm{Cl^-}]}{[\mathrm{Ss}\cdot\mathrm{H^+}]}. \qquad [8, 16]$$

This contradiction only exists if the autoprotolysis equilibrium constant is taken to be constant. If this constant is higher at the surface than in the bulk by three orders of magnitude or more, then this contradiction disappears. In other words, our model of surface adsorption and charge formation remains consistent if the surface also acts to catalyze the autoprotolysis reaction of the ethanol–water solvent.

This is not a large jump to make given that the first step of the catalysis reaction has already been proposed as the charging mechanism for the alumina surface in the pure solvent. As proposed above, an ethanol molecule adsorbs to the surface and desorbs as an ethoxide ion, leaving a proton on the surface. This

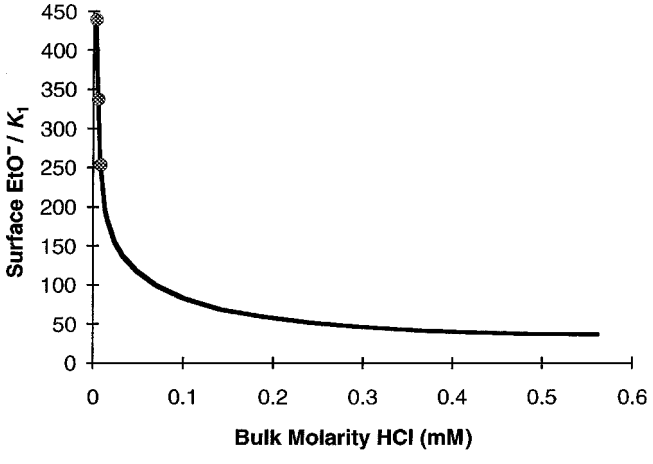

FIG. 11. Relative surface activity of EtO^- ion calculated from surface equilibrium equations [8] and [16].

gives the particles their positive surface charge. The next step would be for some of the protons on the surface to desorb as either hydronium or protonated ethanol ions. These two ions would then diffuse outward a finite distance from the surface and react in solution, re-forming a neutral ethanol molecule. The voltage gradient in the double layer around the particle would accelerate the outward diffusion of the positive ions while retarding the outward diffusion of the ethoxide ions. The outward flux of positive ions from the surface would balance the inward flux of positive ions being consumed by reaction with ethoxide near the surface. The result is that the particle would be able to maintain a layer containing a significant concentration of ethoxide ions even when the bulk solution has a significant proton activity and therefore an effectively zero concentration of ethoxide.

Behavior with Added KOH

Having examined the surface chemical behavior with the addition of a simple acid, we next proceed to add a simple base. Potassium hydroxide was chosen because it was readily available in a low water content ethanol solution. As was mentioned above, potassium hydroxide will react with ethanol, and in a 99.5/0.5 wt% ethanol/water solvent it will convert to 96% potassium ethoxide (18).

Conductivity. In order to measure ionic strengths in solution it is necessary to know the conductivity function for KOH in this concentration of ethanol. Because of the lack of literature data, our first step was to measure the molar conductivity and fit this to the Fuoss–Onsager equation [6]. The curve was fitted to data points taken between concentrations of 1 and 6 mM, which lie in the most accurate measurement range for our system. An iterative fitting algorithm was used which converged unambiguously to the following values: molar limit conductivity, $\Lambda_O = 40.75$; ionic distance of closest approach, $a_O = 3.50$; and ionic association constant, $K_A = 0$. The result is plotted in Fig. 12 along with the data points below 1 mM not used in the fitting.

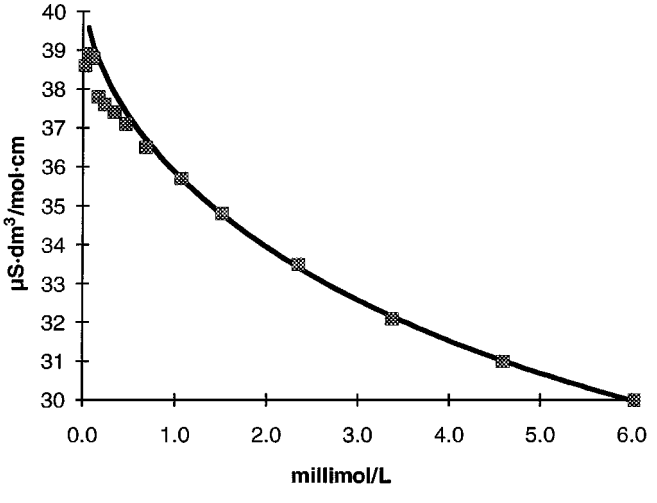

FIG. 12. Molar conductivity of KOH in 99.5/0.5 wt% ethanol/water solvent. Circles are measured data points. Curve is the Fuoss–Onsager equation fitted to data points between 1 and 6 mM.

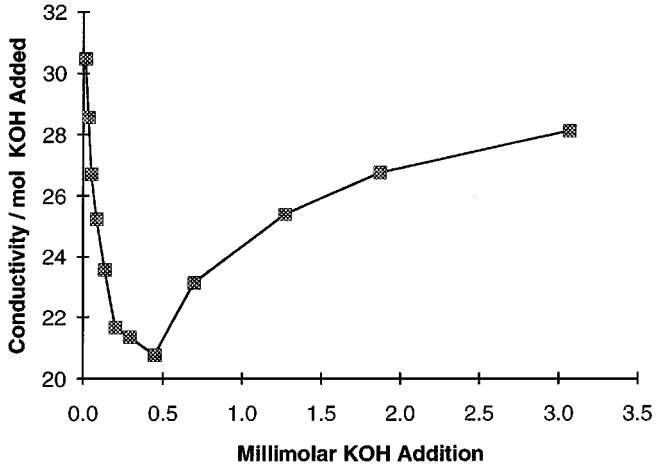

FIG. 13. Conductivity per molar addition of KOH to a 1 vol% alumina suspension.

Adsorption. Adsorption data were obtained by measuring conductivity changes as KOH was titrated into a stirred 1 vol% suspension of alumina powder. The concentration of KOH in solution was determined from conductivity measurements using the Fuoss–Onsager equation with the parameters fitted above. The difference between the KOH in solution and the total KOH added was taken as the powder surface adsorption.

Figure 13 shows the molar conductivity as a function of the total KOH addition to the alumina suspension. This highlights the counterintuitive behavior of adsorption below an addition of 0.4 mM. In this initial region the more KOH that is adsorbed the larger the proportion of additional KOH that will be adsorbed. This is exactly the opposite of what would be expected from a normal adsorption isotherm and can be explained by first understanding the surface charging of the particles.

Zeta potential. As a result of the low surface potentials and consequently low stabilities of alumina suspensions with added KOH, zeta potentials were measured only electroacoustically. Electroacoustic measurements were made in a continuously stirred suspension of 1 vol% alumina powder. An automatic titrator was used to inject a solution of 0.1 molar KOH in 12 μL increments. An unadjusted zeta potential of 44.6 mV was measured before the titrator tip was inserted into the solution.

The bulk ionic strength was used to calculate the Debye length and Henry correction factor for the zeta potential as in the measurements with HCl above. The corrected zeta potential values as a function of bulk KOH concentration are shown in Fig. 14. At a bulk molar concentration of approximately 0.2 mM the indicated zeta potential dropped below zero and went to -1.4 mV at the maximum KOH concentration measured.

Surface charge. With the zeta potential and the bulk ionic strength, the surface charge density can be calculated using

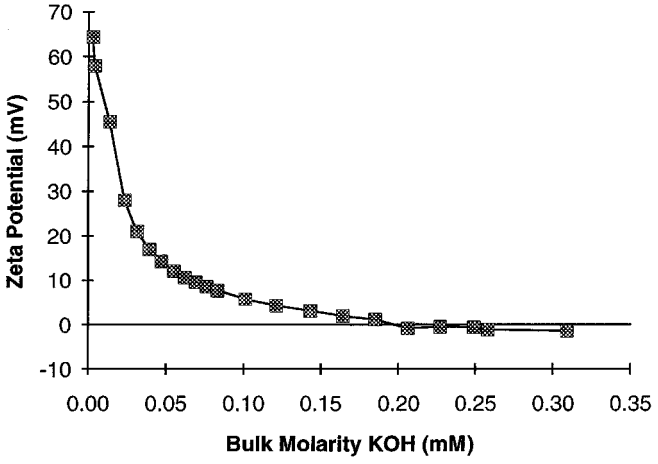

FIG. 14. Zeta potential as a function of molarity of KOH in bulk solution.

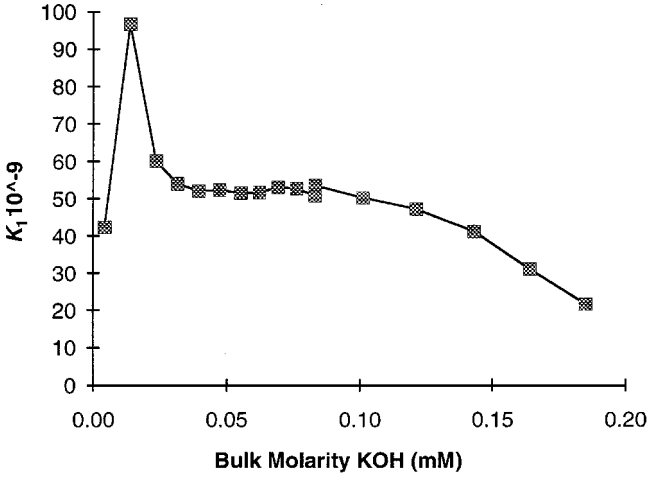

FIG. 16. Plot of K_1 from Eq. [8]. Quantities are in moles or mol/m^2, as appropriate.

Eq. [5]. The results are shown in Fig. 15. The zeta potential is again assumed to be the same as the surface potential.

Modeling surface charge with KOH. Returning to the model for surface charge of alumina in pure ethanol above, we note that ethanol molecules adsorbed to the surface dissociate and ethoxide ions desorb from the surface, leaving a positive surface charge. Knowing the bulk ethoxide activity and zeta potential, the surface ethoxide activity can be calculated using the Boltzmann relation, Eq. [11]. With this it is now possible to plot K_1 from Eq. [8], and this is shown in Fig. 16.

Looking at this plot more closely, it can be seen that if the first three points at the lowest KOH concentrations and the last four points at the highest KOH concentrations can be neglected, then the remaining data points are well within 5% of a constant, as shown in Fig. 17. Moreover, there are very reasonable bases for believing that these points at the extremes can be neglected.

The first three points in Fig. 16 have a relatively high degree of uncertainty both because of uncertainty of the exact quantity titrated in the initial injections of KOH titrant and the uncertainty of the interpolation of free molarity from adsorption data taken in a region where the conductivity is less that 1 μS/cm. Furthermore, if the hypothesis that the surface catalyzes the autoprotolysis of ethanol is correct, then at low ionic strengths in the bulk, the ionic strength at the surface cannot be calculated from the bulk. This adds an additional uncertainty to the surface charge density calculation, which depends on knowing the ionic strength near the surface.

The final four data points plotted in Fig. 16 represent data points where the measured zeta potential is less than 5 mV. There are two easily identifiable sources of error in surface potential measurement at values this low: floccing of the particles and the nature of the surface charge. DLVO calculations

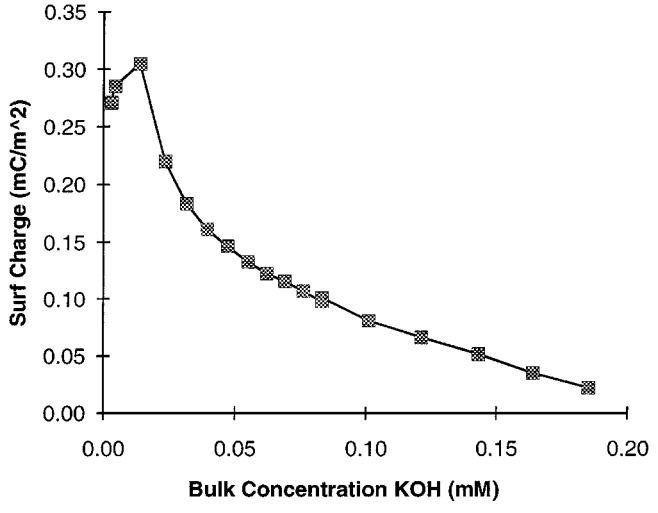

FIG. 15. Surface charge density in millicoulombs per square meter vs bulk concentration of KOH.

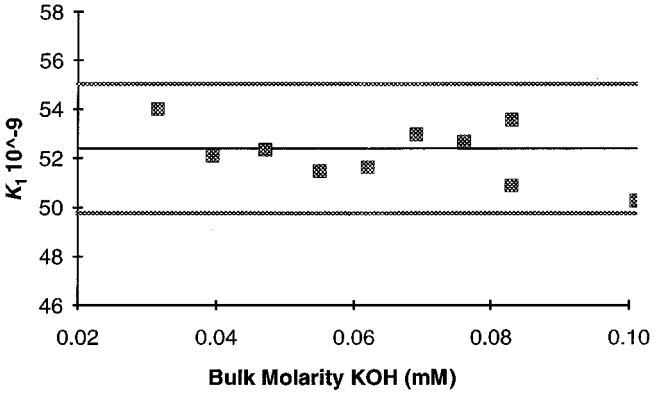

FIG. 17. Plot of K_1 from Eq. [8]. Zeta potentials range from 21 to 5.7 mV; bulk conductivities range from 1.3 to 4.1 μS/cm. The dashed line is the average value of 5.25×10^{-8}. Gray lines indicate $\pm5\%$ from average.

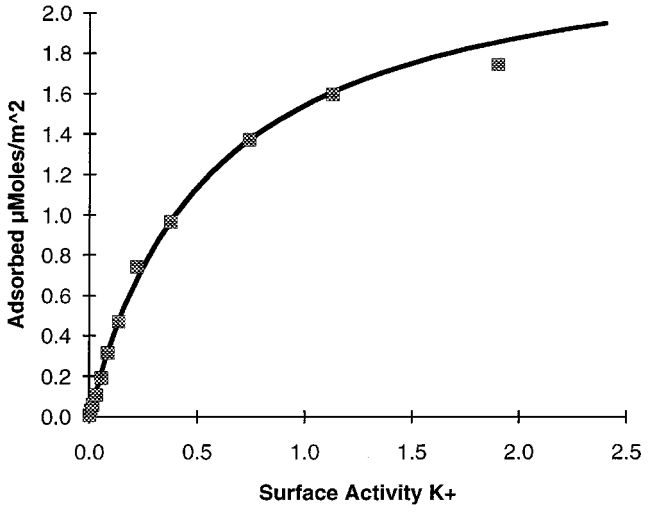

FIG. 18. Surface adsorption as a function of surface K^+ activity.

indicate that the interparticle repulsion goes to zero at a bulk molarity of 0.06. Therefore as zeta potential continues to drop and ionic strength to rise with further additions of KOH, it is reasonable to expect that flocculation of the particles would cause the measured zeta potential to deviate from the actual value beyond this point. Furthermore, at the highest ionic strength/lowest zeta potential point in Fig. 18, the uniform surface charge assumption implicit in the calculations performed here becomes questionable. At this point the zeta potential is 5.7 mV and the bulk ionic strength is 0.10 mM; this gives a surface charge density of 8.1×10^{-5} C/m^2 and a Debye length of 17 nm. If the charge sites are uniformly distributed across the surface, this gives a charge–charge separation distance of 46 nm, almost three times the Debye length.

So, if the hypothesis is that the equilibrium of Eq. [8] describes the particle surface charge, the test of this hypothesis is whether the value of K_1 calculated from measured data is a constant. Given the above arguments, the range of data that supports the contention that K_1 is a constant, as shown in Fig. 17, is actually better than might be expected.

Adsorption of KOH. As can be seen from Fig. 13, the marginal adsorption of KOH increases with increasing KOH concentration. This is only possible if adsorption is mediated by the positive K^+ ion. With the initial small additions of KOH, the positive surface potential repels the positive ions and little adsorption occurs. As more KOH is added, the surface potential drops and the surface concentration of K^+ rises many times faster than the concentration in the bulk. This leads to the inverse marginal adsorption behavior in the region where the particles have a positive and declining surface charge, as illustrated in Fig. 13.

Without making any assumptions about the nature of the surface adsorption site for the potassium ion, the adsorption can be written as an equilibrium with a generic surface site Ss′ as

$$\mathrm{Ss}' + \mathrm{K}_\mathrm{S}^+ \rightleftharpoons \mathrm{Ss}' \cdot \mathrm{K}^+, \qquad K_\mathrm{K} = \frac{[\mathrm{Ss} \cdot \mathrm{K}^+]}{[\mathrm{Ss}']\gamma_+[\mathrm{K}_\mathrm{S}^+]}. \quad [24]$$

This can be rewritten in the form of a standard Langmuir adsorption isotherm,

$$[\mathrm{Ss} \cdot \mathrm{K}^+] = \mathrm{Ss}_\mathrm{Tot} \frac{K_\mathrm{K}\gamma_+[\mathrm{K}_\mathrm{S}^+]}{1 + K_\mathrm{K}\gamma_+[\mathrm{K}_\mathrm{S}^+]}. \quad [25]$$

As above in the case of Cl^- adsorption, the inverse of Eq. [25] is plotted and a straight line is fitted to the data by least squares. The result is a total surface adsorption of 2.4 μmol/m^2 and an adsorption equilibrium constant K_K of 1.8 with quantities in millimolar or millimoles/m^2. The data along with the fitted isotherm are shown in Fig. 18.

What is interesting about this adsorption isotherm is that it appears to be a function only of the surface activity of the positively charged potassium ion and yet has no effect on the surface charge density. Over the concentration range shown in Fig. 17 where surface charge appears to be only a function of ethoxide concentration, the adsorption of K^+ goes from 2% to 60% (0.047 to 1.4 μmol/m^2) of total surface sites, and the surface activity goes up by a factor of 70, from 0.011 to 0.75 mM. From this it is clear that the adsorption of K^+ must be by some charge-neutral mechanism. The adsorption of a K^+ ion must either be accompanied by the adsorption of a negative ion or the desorption of a positive ion and must occur in such a manner that it does not affect the ethoxide adsorption equilibrium.

One possible explanation for the absence of an effect of the K^+ adsorption on surface charge would be that the K^+ could only stably adsorb along with a negative ethoxide or hydroxide ion:

$$\mathrm{Ss}' + \mathrm{K}_\mathrm{S}^+ + \mathrm{EtO}_\mathrm{S}^- \rightleftharpoons \mathrm{Ss}' \cdot \mathrm{K}^+ \cdot \mathrm{EtO}^-. \quad [26]$$

However, this implies a dependency of adsorption on the ethoxide activity at the surface, which is not supported by the data.

Another charge-neutral mechanism would be the substitution of a potassium ion for the proton from a surface adsorbed ethanol molecule:

$$\mathrm{Ss} \cdot \mathrm{H}^+ \cdot \mathrm{EtO}^- + \mathrm{K}_\mathrm{S}^+ \rightleftharpoons \mathrm{Ss} \cdot \mathrm{K}^+ \cdot \mathrm{EtO}^- + \mathrm{H}_\mathrm{S}^+ \quad [27]$$

An argument against this mechanism would be that there should be an effect of the activity of the proton in the solution at the surface. This means that the adsorption should be a function of both the K^+ activity and the inverse of the ethoxide activity, but here again there is no indication of an ethoxide dependency in the data.

However, if we accept the hypothesis that the surface acts as a catalyst to dissociate ethanol molecules into adsorbed protons

and ethoxide ions, then the adsorbed proton concentration will be a function of ethanol activity, which is effectively constant. This mechanism can then fulfill the two seemingly contradictory conditions that: 1. adsorption is only a function of activity of the positive potassium ion and 2. the adsorption of the K^+ ion has no effect on the surface charge, which remains only a function of the ethoxide activity.

A second possible argument against this adsorption mechanism is that the number of sites does not match the number of sites determined by Cl^- adsorption. The total K^+ adsorption is 2.4 μmol/m^2 vs a Cl^- adsorption of 3.5 μmol/m^2. This can potentially be explained by the size difference of the proton and the K^+ ion. An adsorption site density of 3.5 μmol/m^2 would give a site–site spacing of 7.4 Å assuming a uniform hexagonal spacing of sites across the surface. Given that the sites are likely not uniformly spaced, it seems reasonable that there would be sites that would not fit the 3.0 to 3.3 Å diameter K^+ ion.

An implication of this adsorption mechanism and the lack of an effect of K^+ adsorption on the surface charge is that the positive and negative surface adsorption sites are separate sites and do not interact. There has to be a significant physical separation between positive and negative sites for the substitution of the much larger potassium ion to have no effect on the ethoxide adsorption. This in turn implies that surface adsorbed ethanol is completely dissociated into ethoxide and a proton adsorbed to different sites. This again supports the picture of the alumina surface as a catalyst for the autoprotolysis of the ethanol–water solvent.

SUMMARY AND CONCLUSIONS

The picture of the behavior of the alumina surface in ethanol that emerges from the data above is as follows.

When the alumina powder is put into ethanol it adsorbs a coating of ethanol molecules. This is a dissociative adsorption process in which a proton is adsorbed to a Lewis base site and an ethoxide ion is adsorbed to an adjacent Lewis acid site. The dissociated ethanol will also desorb from the surface as negative ethoxide ions and protons in the form of hydronium or protonated ethanol ions. The alumina surface therefore acts as a catalyst for the autoprotolysis reaction of ethanol–water,

$$\begin{aligned} &\mathrm{HEtO} + \mathrm{H_2O} \rightleftharpoons \mathrm{EtO^-} + \mathrm{H_3O^+} \\ &\text{or} \qquad 2\mathrm{HEtO} \rightleftharpoons \mathrm{EtO^-} + \mathrm{H_2EtO^+}. \end{aligned} \tag{22}$$

This behavior is critical to understanding the surface adsorption and surface charging of the alumina powder.

As the two types of ion diffuse outward from the surface they will recombine to form neutral ethanol molecules until at some distance from the particle they reach the equilibrium prevailing in the bulk solution. The effect of this is that the particle surrounds itself with its own ionic atmosphere. At the particle surface there can be significant concentrations of ethoxide ions even when they are virtually nonexistent in the bulk solution.

Of the two ions, the ethoxide ion is more readily dissolved from the surface. This leaves behind a net positive charge on the particles in pure ethanol. When HCl is titrated into the suspension the activity of the ethoxide in the bulk drops effectively to zero due to reaction with the acid. This reduces but does not eliminate the ethoxide in solution at the surface. The reduction of ethoxide in solution at the surface does mean that more ethoxide desorbs from the surface and the net positive charge on the surface increases. The positive charge increases until it begins to be suppressed by the increasing concentration of Cl^- at the surface.

The Cl^- ions are adsorbed at the same Lewis acid sites as the ethoxide ions on the surface. This leads to a competitive adsorption process where the ratio of Cl^- to EtO^- adsorbed to a fixed number of sites on the surface is determined by the activity ratios of the two ions in solution at the surface.

The adsorption energy of the Cl^- ion to these sites is lower than that of the EtO^- ion. Therefore the number of unoccupied sites, which determines surface charge, will be higher at a given concentration of Cl^- compared to the EtO^- ion. This is seen in the very rapid suppression of surface charge with the addition of very small quantities of potassium hydroxide/ethoxide.

The strongest base in ethanol is the ethoxide ion. Any stronger base will react with the ethanol solvent to form ethoxide ions. In the titration of potassium hydroxide/ethoxide the increased concentration of ethoxide in solution suppressed the dissociation of ethoxide from the surface, eliminating the net positive charge on the particle surface. However, despite a significant concentration of free ethoxide in the solvent, the desorption of protons from the surface never significantly exceeded the desorption of ethoxide and no net negative charge formed within the probable margin of error of the measurements made here. Thus it appears unlikely that in the absence of specific adsorption this hydrated alumina will develop a negative surface charge in this solvent.

The objective of this study was to better understand the surface chemical behavior of an oxide powder in a particular system for electrophoretic deposition, with the ultimate goal of being able to quantitatively predict adsorption and surface charge in an arbitrary chemical environment. Based on the formulae and quantities developed in this paper, we are now able to make quantitative estimates of the particle–electrode double layer interaction for many conditions during electrophoretic deposition, and can at least qualitatively describe the interactions at all times and positions in the depositing layer.

APPENDIX

Fundamental Constants

e	elementary charge (1.602×10^{-19} C)
k	Boltzmann constant (1.381×10^{-23} J/K)
ε_o	permitivitty of free space (8.854×10^{-12} C^2/J $\cdot$ m)

General Symbols

a particle radius (m)
a_O geometric mean distance of closest approach of ions in solution (nm)
E Reduced electrophoretic mobility (nondimensional)
EtO^- ethoxide ion
HEtO ethanol molecule
q surface charge density (C/m^2)
Ss surface adsorption site
T temperature (K)
u_E particle electrophoretic mobility ($\mu m \cdot cm/V \cdot s$)
z ion valence
γ_- activity coefficient for negative ion at particle surface
γ_+ activity coefficient for positive ion at particle surface
$\gamma_\pm$ activity coefficient for ions in bulk solution
ε_r relative dielectric constant
η solvent viscosity (poise)
κ inverse Debye length (m^{-1})
ρ_∞ density of dissociated molecules of a binary salt in bulk solution (m^{-3})
ζ particle potential at shear layer (mV)
$\tilde{\zeta}$ reduced particle potential at shear layer (nondimensional)

Conductivity

Λ molar conductivity ($\mu S \cdot dm^3/cm \cdot M$)
Λ_O molar limit conductivity ($\mu S \cdot dm^3/cm \cdot M$)
c molar concentration of dissolved salt (mol/dm^3)
α dissociated fraction of dissolved salt
K_A association constant for oppositely charged ions in solution

Electroacoustics

δ pressure wave decay parameter for acoustophoresis
ω measurement frequency in acoustophoresis (s^{-1})
ρ solvent density in acoustophoresis

ACKNOWLEDGMENTS

The authors thank the Penn State Particulate Materials Center and its member companies for support of this work, in particular Professor James Adair, Dr. Ulrich Eisele, and Dr. Eric Minford for their support in allowing this work to continue, and Dispersion Technology, Inc. for assistance in making electroacoustic measurements.

REFERENCES

1. Hamaker, H. C., and Verwey, E. J. W., *Trans. Faraday Soc.* **36,** 180 (1940).
2. Koelmans, H., and Overbeek, J. Th. G., *Discuss Faraday Soc.* **18,** 52 (1954).
3. Malkin, E. S., and Dukhin, A. S., *Colloid J. USSR* **42,** 396 (1980).
4. Sarkar, P., and Nicholson, P. S., *J. Am. Ceram. Soc.* **79,** 1987 (1996).
5. Parks, G. A., *Chem. Rev.* **65,** 177 (1965).
6. Romo, L. A., *Discuss. Faraday Soc.* **42,** 232 (1966).
7. Lind, J. E., Jr., Zwolenik, J. J., and Fuoss, R. M., *J. Am. Chem. Soc.* **81,** 1557 (1959).
8. Graham, J. R., Kell, G. S., and Gordon, A. R., *J. Am. Chem. Soc.* **79,** 2352 (1957).
9. Kay, R. L., *J. Am. Chem. Soc.* **82,** 2099 (1960).
10. De Lisi, R., Goffredi, M., and Liveri, V. T., *J. Chem Soc. Faraday, Trans. 1* **72,** 436 (1976).
11. Fuoss, R. M., Onsager, L., and Skinner, J. F., *J. Phys. Chem.* **69,** 2581 (1965).
12. O'Brien, R. W., and White, L. R., *J. Chem. Soc. Faraday, Trans.2* **74,** 1607 (1978).
13. Dukhin, A. S., Goetz, P. J., Wines, T. H., and Somasundaran, P., *Colloids Surf. A* **173,** 127 (2000).
14. Sawatzky, R. P., and Babchin, A. J., *J. Fluid Mech.* **246,** 321 (1993).
15. Henry, D. C., *Proc. R. Soc. London Ser. A* **133,** 106 (1931).
16. Loeb, A. L., Overbeek, J. Th. G., and Wiersma, P. H., "The Electrical Double Layer around a Spherical Colloidal Particle." MIT Press, Cambridge, MA, 1961.
17. Popovych, O., and Tomkins, R. P. T., "Nonaqueous Solution Chemistry." Wiley Interscience Publications, New York, 1981.
18. Caldin, E. F., and Long, G., *J. Chem. Soc.* 3737 (1954).